QUANTIZED-STATE CONTROL OF LINEAR SYSTEMS

Ernesto Kofman

Laboratorio de Sistemas Dinamicos. FCEIA - Universidad Nacional de Rosario. Riobamba 245 bis - (2000) Rosario

Abstract: This paper study the main theoretical properties of Quantized State Control (QSC) applied to linear time invariant (LTI) systems. Using a previous result on perturbed systems, a closed formula for the quantization design is deduced. It is shown that the mentioned formula ensures that the difference between the trajectories of the Continuous Control System (CCS) and the QSC system is bounded by a constant which stands even in presence of piecewise constant input references. Finally, the use and advantages of the results are illustrated and discussed through the simulation of some examples.

Keywords: Digital Control, Quantization Effects, Discrete Event Systems.

1. INTRODUCTION

Quantized State Control (Kofman, 2001a,b) is a methodology which allows the digital implementation of previously designed continuous controllers based on the quantization of their state variables. The resulting digital controller –which can be described by a discrete event system– is completed with an asynchronous sampling scheme so that, ignoring the temporal errors introduced by the clock of the digital device, no time discretization is performed.

The advantages of QSC are related with the conservation in the digital implementation of the regional an even global stability properties achieved by the continuous controller and with the reduction of the computational costs and the quantization effects introduced by the A/D and D/A converters. The general properties of QSC proven in (Kofman, 2001a) tell that when the CCS has an asymptotically stable equilibrium point, a quantization can be found so that the resulting QSC system trajectories are ultimately bounded by an arbitrary small region around that equilibrium point and so that the region of attraction is conserved. This result, based on a Lyapunov's analysis, also gives an algorithm to compute the quantization to be applied.

A first remark is that the term *stability* is changed by *ultimately boundedness* of the solutions (Khalil, 1996). This seems to be a disadvantage with respect to classic discrete time controllers which usually guarantee asymptotic stability. However, when the quantization effects of the converters are taken into account, the asymptotic stability also disappears from these control systems and the utimately boundedness is the only thing which can be ensured (Miller et al., 1988; Farrel and Michel, 1989; Hou et al., 1997).

In this work, the particular case of LTI QSC systems is studied. This particularization allows replacing the Lyapunov-based algorithm by a formula which relates the quantization applied with the ultimate bound obtained. Based on a result of (Kofman, 2002), it is also proven that this quantization produces that the difference between the CCS and the QSC system trajectories is never greater than the mentioned bound, even in presence of piecewice constant references.

The work is organized as follows. In Section 2 the basic principles and definitions of QSC are introduced. Then, the particular case of LTI systems is considered in Section 3, where the study of the error bound is performed. Finally, in Section 4 two examples are discussed, showing not only the use of the mentioned closed formula but also some advantages over the classic digital control scheme.

2. QUANTIZED STATE CONTROL

Quantized State Control is based on the addition of hysteretic quantization functions to a continuous controller. Before recalling the QSC definition, the hysteretic quantization functions will be introduced.

2.1 Quantization Functions

Let $D = \{d_0, d_1, ..., d_r\}$ be a set of real numbers where $d_{i-1} < d_i$ with $1 \leq i \leq r$ and let $x \in \Omega$ be a continuous trajectory, where $x : \mathbb{R} \to \mathbb{R}$. Let $b : \Omega \times t_0 \to \Omega$ be a mapping and let $q = b(x, t_0)$ where the trajectory q for $t \geq t_0$ satisfies

$$q(t) = \begin{cases} d_m & \text{if } t = t_0 \\ d_{i+1} & \text{if } x(t) = d_{i+1} \wedge q(t^-) = d_i \\ & \wedge i < r \\ d_{i-1} & \text{if } x(t) = d_i - \varepsilon \\ & \wedge q(t^-) = d_i \wedge i > 0 \\ q(t^-) & \text{otherwise} \end{cases} \tag{1}$$

and

$$m = \begin{cases} 0 & \text{if } x(t_0) < d_0 \\ r & \text{if } x(t_0) \geq d_r \\ j & \text{if } d_j \leq x(t_0) < d_{j+1} \end{cases}$$

Then, the map b is a *Quantization Function with Hysteresis*. The width of the hysteresis window is ε. The values d_0 and d_r are the lower and upper saturation values. Figure 1 shows a typical quantization function with uniform quantization intervals. A fundamental

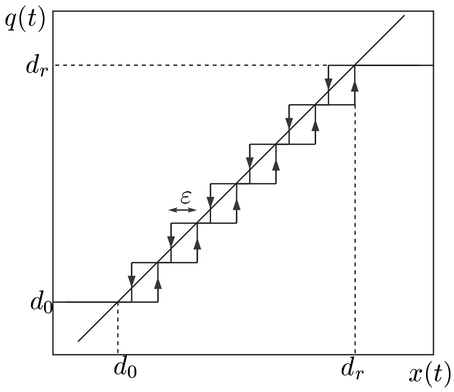

Fig. 1. Quantization Function with hysteresis

property of a Quantization Function with hysteresis when $t \geq t_0$ and $d_0 \leq x(t) \leq d_r$ is given by the following inequality

$$|q(t) - x(t)| \leq \max_{1 \leq i \leq r}(d_i - d_{i-1}, \varepsilon) \tag{2}$$

2.2 Quantized State Systems

Consider the State Equation System given by:

$$\begin{cases} \dot{x}(t) = f(x(t), u(t)) \\ y(t) = g(x(t), u(t)) \end{cases} \tag{3}$$

Related to this system, an associated Quantized State System (QSS) (Kofman and Junco, 2001) is defined as follows:

$$\begin{cases} \dot{x}(t) = f(q(t), u(t)) \\ y(t) = g(q(t), u(t)) \end{cases} \tag{4}$$

where $q(t)$ and $x(t)$ are related (componentwise) by quantization functions with hysteresis. The components of the vector $q(t)$ are called *quantized variables*.

The most significant properties of the QSS are related to the form of the trajectories. Provided that the inputs have piecewise constant trajectories and the function f is continuous and bounded in any bounded domain, the following properties are satisfied:

- The quantized variables have piecewise constant trajectories
- The state variable derivatives have also piecewise constant trajectories
- The state variables have continuous piecewise linear trajectories

As a consequence of these properties the QSS can be exactly simulated by a discrete event model within the DEVS formalism framework (Zeigler et al., 2000). The DEVS model related to a generic QSS, the proof of the mentioned properties and an extended explanation about the necessity of using hysteresis can be found in (Kofman and Junco, 2001).

The possibility of representing a QSS by a DEVS model and the fact that DEVS models can be simulated in real time by digital devices (Zeigler and Kim, 1993) allow the use of QSS as digital controllers.

2.3 QSC Definition

Consider the CCS consisting of plant and controller, Eqs. (5) and (6) respectively, and their (ideal) interconnection, Eq. (7).

$$\begin{cases} \dot{x}_p(t) = f_p(x_p(t), u_p(t)) \\ y_p(t) = g_p(x_p(t)) \end{cases} \tag{5}$$

$$\begin{cases} \dot{x}_c(t) = f_c(x_c(t), u_c(t), u_r(t)) \\ y_c(t) = g_c(x_c(t), u_c(t), u_r(t)) \end{cases} \tag{6}$$

$$u_p(t) = y_c(t), \quad u_c(t) = y_p(t) \tag{7}$$

Note that $u_r(t)$ represents an input reference.

Definition 1. A QSS associated to a continuous controller (6) is called Quantized State Controller (QSC controller).

Definition 2. A QSC system is defined as a control scheme composed by a continuous plant and a QSC controller connected through asynchronous A/D and D/A converters.

Figure 2 shows a block diagram representation of a QSC system. The QSC implementation of the controller transforms (6) into the new set of equations:

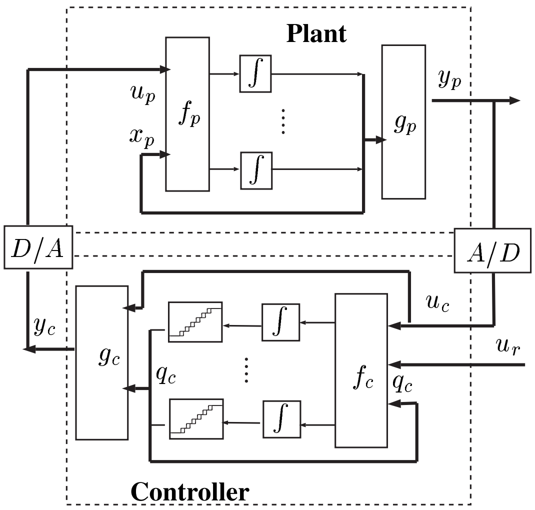

Fig. 2. Block Diagram of the QSC system

$$\begin{cases} \dot{x}_c(t) = f_c(q_c(t), u_c(t), u_r(t)) \\ y_c(t) = g_c(q_c(t), u_c(t), u_r(t)) \end{cases} \quad (8)$$

where the difference between the components of q_c and x_c is bounded according to (2).

The asynchronous sampling scheme (Sayiner et al., 1993) implies that the A/D conversions are performed only when the analog input and the digital output of the converters differ in a quantity corresponding to one quantization interval. Then, they can be seen as quantization functions with hysteresis where the quantization intervals and the hysteresis windows have the same size. In a similar way, the D/A converters can be represented by quantization functions without hysteresis ($\varepsilon = 0$). Thus, the presence of the asynchronous converters transforms (7) into:

$$u_p(t) = y_{c_q}(t), \;\; u_c(t) = y_{p_q}(t) \quad (9)$$

where the variables $y_{c_q}(t)$ and $y_{p_q}(t)$ are the quantized versions of the plant and the controller output variables, which differ from the continuous y_c and y_p in a quantity bounded by (2).

3. LTI QUANTIZED STATE CONTROL

3.1 Closed-Loop Equations

Consider the Continuous LTI plant (10) and controller(11).

$$\begin{cases} \dot{x}_p(t) = A_p x_p(t) + B_p u_p(t) \\ y_p(t) = C_p x_p(t) \end{cases} \quad (10)$$

$$\begin{cases} \dot{x}_c(t) = A_c x_c(t) + B_c u_c(t) + B_r u_r(t) \\ y_c(t) = C_c x_c(t) + D_c u_c(t) + D_r u_r(t) \end{cases} \quad (11)$$

With the interconnection given by (7), the following closed loop equation is obtained.

$$\dot{x}(t) = Ax(t) + Bu_r \quad (12)$$

where

$$x(t) = \begin{bmatrix} x_p(t) \\ x_c(t) \end{bmatrix}, \quad A = \begin{bmatrix} A_p + B_p D_c C_p & B_p C_c \\ B_c C_p & A_c \end{bmatrix}$$

and

$$B = \begin{bmatrix} B_p D_r \\ B_r \end{bmatrix}$$

The QSC implementation of the controller modifies (11) which can be rewritten as

$$\begin{cases} \dot{x}_c = A_c(x_c + \Delta x_c) + B_c u_c + B_r u_r \\ y_c = C_c(x_c + \Delta x_c) + D_c u_c + D_r u_r \end{cases} \quad (13)$$

where Δx_c expresses the difference between the state variable and its quantized version. In a similar way, the effects of the A/D and D/A asynchronous converters in (9) can be also described by the following equations:

$$u_c(t) = y_p(t) + \Delta y_p(t), \; u_p(t) = y_c(t) + \Delta y_c(t)$$

Thus, taking into account (10),(13) and the last equation, the use of the QSC scheme transforms equation (12) into

$$\dot{x} = A(x + \Delta x) + F\Delta y + Bu_r \quad (14)$$

where

$$\Delta x = \begin{bmatrix} 0 \\ \Delta x_c \end{bmatrix}, \Delta y = \begin{bmatrix} \Delta y_p \\ \Delta y_c \end{bmatrix}, F = \begin{bmatrix} B_p D_c & B_p \\ B_c & 0 \end{bmatrix} \quad (15)$$

3.2 Error in LTI QSC

Let $x(t)$ and $\tilde{x}(t)$ and be solutions of (12) and (14) starting from the same initial condition $x(t_0) = \tilde{x}(t_0) = x_0$. Then the error

$$e(t) = \tilde{x}(t) - x(t) \quad (16)$$

can be seen as a bound for the lost of performance due to the QSC implementation.

From (12), (14), (16) and the definitions of $x(t)$ and $\tilde{x}(t)$ we have

$$\dot{e}(t) = A[e(t) + \Delta x(t)] + F\Delta y(t)$$
$$e(t_0) = 0$$

Since the components of Δx and Δy are bounded by the corresponding quantum size adopted, Theorem 1 of (Kofman, 2002) can be applied in order to quantify the error due to the QSC scheme. That theorem gives a bound which is usually much less conservative than the given by a classic Lyapunov-based perturbation analysis.

Theorem 1. Let $x(t)$ and $\tilde{x}(t)$ be trajectories of a LTI CCS and its QSC implementation starting from the same initial condition and let A be the evolution matrix of the continuous closed loop system. If A is Hurwitz and diagonalizable, the difference between both trajectories is always bounded by

$$|\tilde{x}(t) - x(t)| \leq |V| \left(|\mathbb{R}\mathrm{e}(\Lambda)^{-1}\Lambda||V^{-1}|\Delta q_x + \right.$$
$$\left. + |\mathbb{R}\mathrm{e}(\Lambda)^{-1}V^{-1}F|\Delta q_y \right) \quad (17)$$

where[1] Δq_x is the vector of quantum sizes in the plant and controller state variables (all the components corresponding to the plant are zero), Δq_y is the vector of quantum sizes in the plant and controller output variables (introduced by the A/D and D/A converters respectively), the matrix F is defined according to (15), Λ is a diagonal matrix of eigenvalues of A and V is a corresponding matrix of eigenvectors.

The proof is straightforward using the mentioned theorem. Inequality (17) can be used as a design formula to obtain the quantization in the controller and converters according to the deviation allowed from the CCS trajectories.

A very important remark is that the mentioned bound does not depend on the initial condition or in the reference trajectory ($u_r(t)$). The only restriction is that $u_r(t)$ must be piecewise constant in order to guarantee that the QSC can be exactly represented by a DEVS model and then implemented on a digital device.

4. EXAMPLES AND RESULTS

4.1 A PI controller example

Consider the plant (5) with

$$A_p = \begin{bmatrix} 0 & 1 \\ -1 & -4 \end{bmatrix}, B_p = \begin{bmatrix} 0 \\ 1 \end{bmatrix}, C_p = \begin{bmatrix} 1 & 0 \end{bmatrix} \quad (18)$$

A PI controller with parameters K_P and K_I can be written in the form of (6) with $A_c = 0$, $B_c = -1$, $B_r = 1$, $C_c = K_I$, $D_c = -K_P$ and $D_r = K_P$. Thus, using $K_P = K_I = 10$, the closed loop evolution matrix is

$$A = \begin{bmatrix} 0 & 1 & 0 \\ -11 & -4 & 10 \\ -1 & 0 & 0 \end{bmatrix}$$

A possible matrix of eigenvectors is

$$V = \begin{bmatrix} 0.0085 + j0.342 & 0.0085 - j0.342 & 0.5452 \\ -0.825 - j0.433 & -0.825 + j0.433 & -0.734 \\ -0.108 + j0.064 & -0.108 - j0.064 & 0.4049 \end{bmatrix}$$

Taking $\Delta q_c = \Delta y_p = 0.01$ and $\Delta y_c = 0.1$, the error bound according to (17) is 0.1443, 0.3383 and 0.0679 in each state variable of the plant and controller respectively. Thus, the maximum error on the plant oputput is bounded by 0.1443. Figure 3 shows the evolution of the plant output with the continuous controller and the QSC controller when the reference is a step of amplitude 10. Figure 4 shows the difference between both trajectories. The maximum difference was 0.1399 which is near the theoretical bound. Here, the use of the Lyapunov based bound gives an error bound of 54.84 which is very conservative.

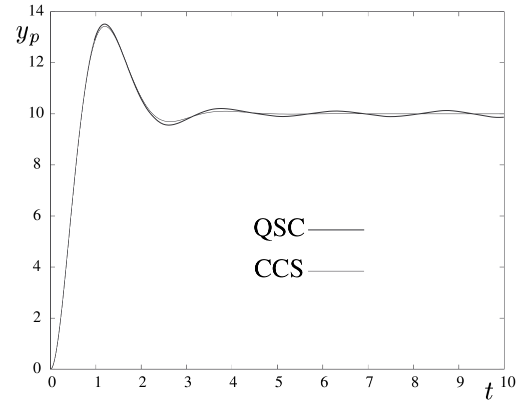

Fig. 3. Plant output with CCS and QSC

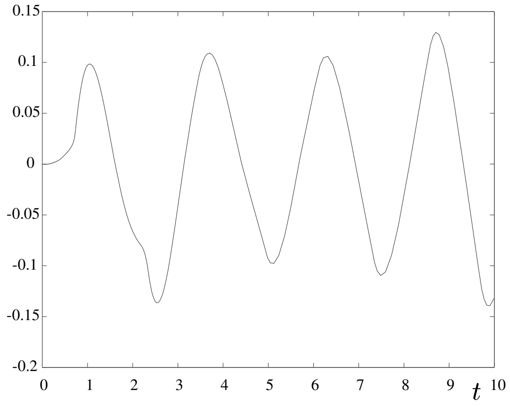

Fig. 4. Difference in the plant output with CCS and QSC

4.2 An inverted pendulum control

The following example was taken from (Messner and Tilbury, 1998). Consider the inverted pendulum of Figure 5 Using parameters $M = 0.5$; $m = 0.2$;

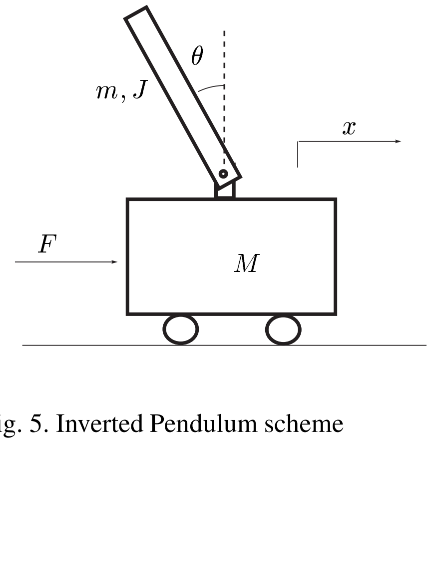

Fig. 5. Inverted Pendulum scheme

[1] The symbol $|\cdot|$ denotes the componentwise modulus of a vector or matrix. For two vectors of thew same dimension a and b, we say $a \leq b$ if the inequality stands for all their components. This implies that (17) expresses a bound for each state variable

$b = 0.1$ (friction of the cart); $J = 0.006$; $g = 9.8$; and $l = 0.3$ (length to pendulum center of mass), a linearized model around $\theta = \pi$ is given by the equations:

$$\begin{bmatrix} \dot{x} \\ \ddot{x} \\ \dot{\Phi} \\ \ddot{\Phi} \end{bmatrix} = \begin{bmatrix} 0 & 1 & 0 & 0 \\ 0 & -0.181 & 2.672 & 0 \\ 0 & 0 & 0 & 1 \\ 0 & -0.454 & 31.18 & 0 \end{bmatrix} \begin{bmatrix} x \\ \dot{x} \\ \Phi \\ \dot{\Phi} \end{bmatrix} + \begin{bmatrix} 0 \\ 1.818 \\ 0 \\ 4.545 \end{bmatrix} u$$

where $\Phi \triangleq \theta - \pi$ is the deviation angle from the vertical position.

The goal is to implement a control for the cart position. The variables measured are x and Φ. Thus, the plant output equations can be written as

$$y = \begin{bmatrix} 1 & 0 & 0 & 0 \\ 0 & 0 & 1 & 0 \end{bmatrix} \begin{bmatrix} x \\ \dot{x} \\ \Phi \\ \dot{\Phi} \end{bmatrix}$$

Messner and Tilbury (1998) arrive to a controller following an LQR design with weights $w_x = 5000$ and $w_\Phi = 100$ and then using a full state observer. For the observer design, the estimator poles were placed at $p_1 = 40$, $p_2 = 41$, $p_3 = 42$ and $p_4 = 43$. In that way, they arrive to a state space controller that can be written in the form of (11), where

$$A_c = \begin{bmatrix} -82.64 & 1 & 1.037 & 0 \\ -1570 & 68.61 & 148.9 & -38.04 \\ 1.385 & 0 & -83.18 & 1 \\ 397.6 & 171.5 & 2209 & -95.11 \end{bmatrix}$$

$$B_c = \begin{bmatrix} 82.64 & -1.037 \\ 1699 & -40.22 \\ -1.385 & 83.18 \\ -76.18 & 1760 \end{bmatrix}; B_r = \begin{bmatrix} 0 \\ -128.6 \\ 0 \\ -3.214 \end{bmatrix}$$

$$Cc = \begin{bmatrix} 70.71 & 37.83 & -1055 & -20.92 \end{bmatrix}$$

and

$$Dc = \begin{bmatrix} 0 & 0 \end{bmatrix}; Dr = -70.71$$

For the QSC digital implementation of the controller, the following quantization sizes were adopted:

$$\Delta q_x = \begin{bmatrix} 0.001 \\ 0.015 \\ 0.002 \\ 0.04 \end{bmatrix}; \Delta q_y = \begin{bmatrix} 0.002 \\ 0.004 \\ 2 \end{bmatrix}$$

The QSC performance was compared with a classic discrete controller obtained from the discretization of the continuous controller. The sampling time of the classic digital controller was taken as $T_s = 0.01$. In this case, we also considered the presence of A/D and D/A converters with the same quantization than in the QSC control (i.e. 0.002 in the position, 0.004 in the angle and 2 in the controller output).

Figures 6-8 show the trajectories obtained with the continuous time controller (without quantization), with the QSC controller and the classic discrete time controller. The first observation is that the QSC shows a much better performance during the transient (see Figure 7) and it reduces the final oscillations.

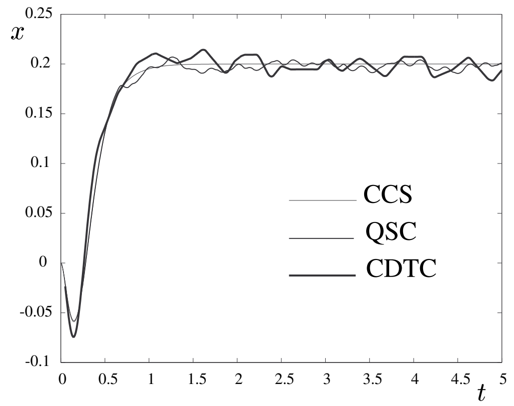

Fig. 6. Cart position with QSC and Classic Digital Control.

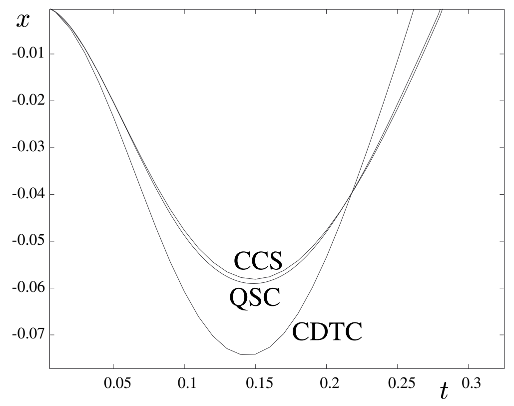

Fig. 7. Cart position (start up) with QSC and Classic Digital Control.

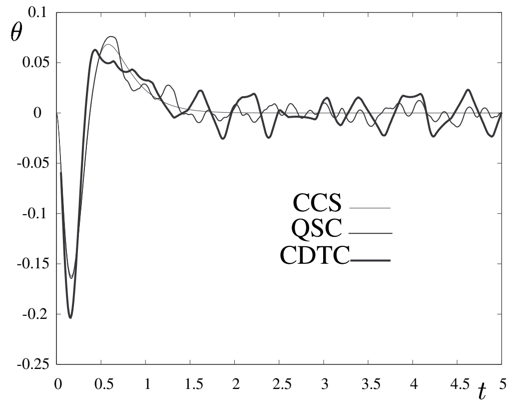

Fig. 8. Pendulum angle with QSC and Classic Digital Control.

The number of A/D conversions performed by the QSC converters in the 5 seconds of simulation was 211 and 185 in the position and angle respectively while the classic digital controller performs $5/0.01 = 500$ conversions in each variable. Similarly, the number of D/A conversions in the QSC control was 303. The classic discrete time controller also performs 500 D/A conversions.

If we take into account what happen from $t = 3$ to $t = 5$ (during the *steady state*), we can see that the QSC only performs 29 A/D conversions in the position, 44 A/D conversions in the angle and 76 D/A conversions while the discrete time controller performs 200 conversions in each variable. The reduction of the computational cost is evident.

These advantages are paid with more calculations at the controller (the number of changes in the internal variables is 1600 against the 500 in the discrete time controller). However, the time required to perform A/D and D/A conversions is always much bigger than the time used for a simple calculation. Anyway, the number of calculations at the controller can be also reduced using a different realization. An interesting alternative is to use a diagonal –or block-diagonal– evolution matrix A_c. In this way, the QSS simulation becomes much more efficient. In one hand, the number of changes in the quantized variables is reduced. In the other hand, each transition involves calculations only in the state which is actually changing (one of the most important features of QSS simulation is that it exploits the sparsity properties). In our example, the use of a block diagonal controller reduces the number of calculations to 547 in 5 seconds obtaining a similar performance.

It is also interesting to observe that the fastest pole of the closed-loop system is placed at 43. Thus, the mean sampling frequencies in the QSC during the *steady state* are below the system bandwidth. Thus, the QSC scheme works violating the Nyquist frequency. It is well known that a sampled data system working below that frequency will be unstable. QSC can work using that frequency because the equilibrium point in the QSC scheme is in fact unstable (but the solutions are ultimately bounded).

Finally, it should be mentioned that the use of inequality (17) gives a quite conservative bound in this case. The error bound in $x(t)$ is 3.08, which is about 300 times bigger than the error observed in Figure (6). Anyway, a Lyapunov analysis gives a bound of 9.6×10^9, which is completely useless for the design.

5. CONCLUSIONS

The properties of the QSC digital implementation of controllers in LTI systems was presented. The main result shows that the difference between the QSC and the original CCS trajectories is always bounded according to the inequality (17). Moreover, this property stands for all initial conditions and piecewise constant input references. The mentioned inequality can be also used as a design equation for the choice of the quantization in the state variables and converters.

Another important quality is the reduction of the computational costs and quantization effects, which were illustrated in an example. All this benefits, and the advantages in nonlinear systems proven in (Kofman, 2001a), convert the QSC scheme in an interesting alternative to the classic discrete time digital implementation.

With respect to future work, the non diagonalizable case should be taken into account. It would be also interesting studying the effects of the time discretization introduced by the clock of the digital device. Finally, the use of non-uniform quantization must be considered since it could result in a very important reduction of the number of calculations performed by the controller.

REFERENCES

J. Farrel and A. Michel. Estimates of asymptotic trajectory bounds in digital implementations of linear feedback control systems. *IEEE Trans. Automat. Contr.*, 34:1319–1324, 1989.

L. Hou, A. Michel, and H. Ye. Some qualitative properties of sampled-data control systems. *IEEE Trans. Automat. Contr.*, 42:1721–1725, 1997.

H. Khalil. *Nonlinear Systems*. Prentice-Hall, New Jersey, 2nd edition, 1996.

E. Kofman. Quantized-State Control. A Method for Discrete Event Control of Continuous Systems. Part I. In *Proceedings of RPIC'01*, pages 103–108, 2001a.

E. Kofman. Quantized-State Control. A Method for Discrete Event Control of Continuous Systems. Part II. In *Proceedings of RPIC'01*, pages 109–114, 2001b.

E. Kofman. Non Conservative Ultimate Bound Estimation in LTI Perturbed Systems. Technical Report LSD0201, LSD-UNR, 2002. Submitted to AADECA'02. Available at www.eie.fceia.unr.edu.ar/∼ekofman/.

E. Kofman and S. Junco. Quantized State Systems. A DEVS Approach for Continuous System Simulation. *Transactions of SCS*, 18(3):123–132, 2001.

William Messner and Dawn Tilbury. *Control Tutorials For MATLAB And Simulink: A Web-Based Approach*. Addison-Wesley, 1998.

R. Miller, M. Mousa, and A. Michel. Quantization and overflow effects in digital implementation of linear dynamic controllers. *IEEE Trans. Automat. Contr.*, 33:698–704, 1988.

N. Sayiner, H. Sorensen, and T. Viswanathan. A non-uniform sampling technique for A/D conversion. In *Proceedings of ISCAS'93*, volume 2, pages 1220–1223, 1993.

B. Zeigler and J. Kim. Extending the DEVS-Scheme knowledge-based simulation environment for real time event-based control. *IEEE Trans. on Robotics and Automation*, 3(9):351–356, 1993.

B. Zeigler, T.G. Kim, and H. Praehofer. *Theory of Modeling and Simulation. Second edition*. Academic Press, New York, 2000.